

Ultra-Fast Health Estimation of Li-ion Batteries Applying Online Internal Impedance Measurement

1st Minh Tran
Electrical Engineering
Tampere University
Tampere, Finland
minh.tran@tuni.fi

2nd Daniel Stroe
AAU Energy
Aalborg University
Aalborg, Denmark
daniel.stroe@aau.dk

3rd Tomi Roinila
Electrical Engineering
Tampere University
Tampere, Finland
tomi.roinila@tuni.fi

Abstract—Lithium-ion (Li-ion) batteries have become the dominant energy storage technology of transportation and various industrial products in recent years. Despite the rapid growth in popularity, Li-ion battery usage faces several challenges such as safety and waste management difficulty. Safe and reliable use of Li-ion batteries depends on accurate state-of-health (SOH) estimation. While studies have shown various techniques of battery health estimation, most require either high computational effort or high cost of implementation. Battery state estimation based on impedance spectroscopy have gained traction in recent years due to many attractive benefits such as direct indication of battery performance and non-destructive measuring approach. Furthermore, online impedance measurement techniques based on broadband perturbations have been shown as a fast and cost-effective alternative to traditional impedance spectroscopy. This paper demonstrates the use of discrete-interval binary sequence (DIBS) method in developing an efficient SOH estimation algorithm for Li-ion batteries based on least-square techniques. Experimental results based on several commercial Li-ion battery cells at various conditions are presented and analyzed. A health prediction error of less than 1% was achieved from the experimental work.

I. INTRODUCTION

The application of Li-ion batteries in transportation, energy production and consumer products have been continuously increasing in recent years. The wide adoption of Li-ion batteries is due to several high-performance properties of lithium ions such as high energy density and high power density [1]. However, safe and reliable operation remain challenging as Li-ion batteries carry highly reactive chemicals and complex electrochemical processes. Li-ion battery applications thus require constant monitoring of state parameters such as the battery state of health (SOH) and temperature in order to maintain a safe and long-lasting operation.

The battery SOH, conventionally defined as the percentage of the current charge capacity against the factory-rated charge capacity, is a direct indication of a battery storage performance. As the battery operates by being charged and discharged, aging processes occur leading to a reduction of SOH over time. A threshold value of 70%-80% is conventionally adopted by automotive industry to indicate the end of Li-ion battery life, after which the battery storage capacity is deemed insufficient for vehicle operation [2].

Accurate SOH estimation allows for in-time detection of end-of-life age limit, ensuring safety and performance of

battery-powered products. In addition, SOH estimation can be used in the sorting process for second-life battery remanufacturing. Despite strong efforts to improve and develop new SOH estimation techniques, accurate and cost-effective implementation of SOH estimation in practical applications remain limited, which can generally be attributed to battery degradation complexities, modeling sensitivity, high computational effort or high cost of implementation [3]–[5].

Studies have shown that internal impedance is an effective indicator for determining the SOH of Li-ion batteries [6]–[8]. Impedance spectroscopy is a non-destructive measurement technique that provides direct information about key battery state parameters. Despite its high predictive accuracy, the application of impedance-based SOH estimation remains largely confined to laboratory research for several reasons. First, conventional impedance measurement methods require expensive equipment and lengthy measurement times, making them impractical for real-world battery applications. Second, SOH estimation using impedance spectroscopy typically involves modeling techniques such as electrochemical modeling or equivalent circuit modeling, which are sensitive to parameter changes over the battery’s lifespan and prone to model fitting errors [4], [5].

Studies have proposed methods based on binary broadband perturbations and Fourier techniques for performing online battery impedance measurements [9]–[11]. Binary excitations offer several advantages over the sinusoidal excitations used in traditional electrochemical impedance spectroscopy (EIS), including lower implementation costs and faster measurement times. However, conventional broadband perturbations, such as the pseudo-random binary sequence (PRBS), are sensitive to noise, which can reduce the accuracy of impedance measurements in practical applications. To address this limitation, recent studies have demonstrated the effectiveness of the discrete-interval binary sequence (DIBS) for onboard battery impedance measurement [12], [13]. DIBS is a computer-optimized binary signal in which the energy of several harmonic frequencies is significantly enhanced without increasing the signal’s time-domain amplitude. As a result, DIBS provides a high level of noise resistance, making it well-suited for practical battery measurement scenarios.

This paper presents a practical method for estimating the

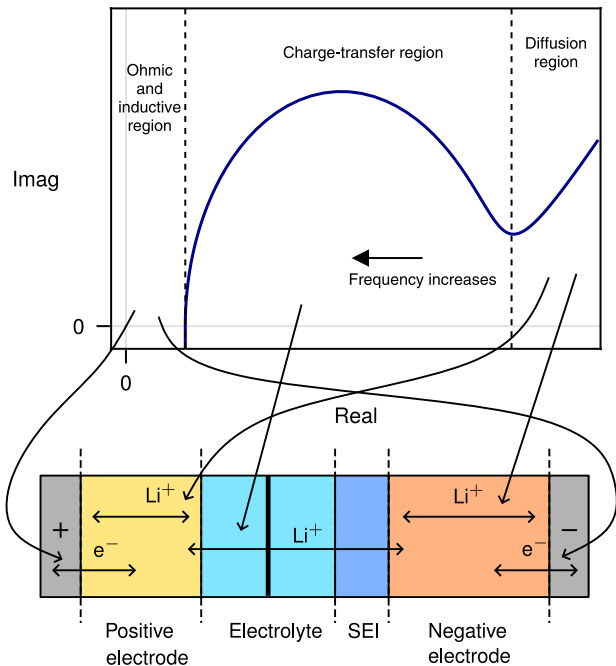


Fig. 1: Li-ion cell internal impedance spectra and charge transportation across different cell layers.

SOH of Li-ion batteries using the DIBS for online impedance measurement. The proposed approach leverages the key advantages of the DIBS, including fast measurement, high accuracy, and minimal system disturbance. To ensure computational efficiency, least-squares and linear modeling techniques are employed, while also accounting for variations in other state parameters such as state of charge (SOC) and temperature.

The remainder of the paper is organized as follows. Section II provides the theoretical background on the relationship between Li-ion battery health and internal impedance. Section III outlines the proposed methodology. Section IV presents experimental measurements conducted on several commercial Li-ion batteries and applies the proposed method to estimate battery health. Finally, Section V concludes the paper.

II. THEORY

Studies have shown that the internal impedance provides key information about a Li-ion battery dynamic processes [14]. The impedance is typically represented as a complex-value function in the frequency domain as $Z = R + jX$, where R is the real part of the impedance that describes the resistive characteristic and X is the imaginary part of the impedance that describes the reactive characteristic. Fig. 1 shows a typical impedance spectra of a Li-ion battery cell as a Nyquist plot. The imaginary axis is inverted to show the capacitive characteristic in the first quadrant of the diagram.

The impedance spectra can be divided into several regions that describe the movement of charges at different parts of the cell. At low frequencies of less than a few hundred

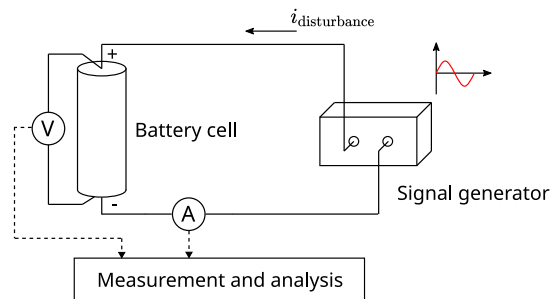


Fig. 2: Battery impedance measurement setup.

mHz, a 45° tilted line in the impedance spectra describes the diffusion of Li-ions in the electrodes. The mid-frequency region, which usually ranges from several mHz to a few kHz, describes the charge transfer kinetics of Li-ions in between the solid-electrolyte interphase (SEI) layer, the electrolyte and the electrodes. At higher frequencies, ohmic and inductive behaviors dominate and characterize the electronic flow in the outer conductive parts of the cell.

Li-ion battery aging is driven by various naturally occurring degradation processes, such as the corrosion of electrode materials, the thickening of the SEI layer, and electrolyte depletion [15]–[17]. External factors like high load currents and elevated temperatures further accelerate these degradation mechanisms. Among them, the growth of the SEI layer—formed at the interface between the negative electrode and the electrolyte—has been identified as the dominant cause of battery capacity loss over time [15], [18], [19]. This SEI buildup results in increased internal resistance and double-layer capacitance, which is typically reflected as an enlarged semicircular arc in the Nyquist plot of the impedance spectrum.

III. METHODS

A. Broadband impedance measurement

The battery impedance is conventionally obtained by applying an EIS [20]. In EIS, sinusoidal excitation currents at multiple frequencies are sequentially injected into the test battery, as shown in Fig. 2. The EIS method provides accurate impedance measurement results; however, applying sinusoidal excitations requires a relatively long measurement time. Moreover, sinusoids contain a large number of signal levels, making signal generation challenging in practice, especially when cost minimization is a priority.

Recent studies have demonstrated that broadband perturbation methods, such as the pseudo-random binary sequence (PRBS), can measure battery impedance in a fraction of the time required by conventional electrochemical impedance spectroscopy (EIS) [9]–[11]. PRBS is a widely used binary signal that distributes spectral energy across multiple harmonic frequencies. Its binary nature makes it easy to generate using low-cost electronic components. In the frequency domain, PRBS exhibits a nearly uniform energy distribution across the spectrum, enabling full spectral coverage with a single signal injection. Consequently, impedance measurements using

PRBS can be completed much faster than those using traditional EIS.

B. Discrete-interval binary sequence

Applying PRBS in practical battery applications poses a challenge due to the signal's high sensitivity to noise. This issue arises from the broad distribution of the signal's total energy across a large number of harmonic frequencies in the measurement spectrum. Onboard battery impedance measurement is especially vulnerable to noise disturbances, given the small magnitude of Li-ion battery impedance and the presence of significant electromagnetic interference. Although increasing the PRBS injection amplitude can reduce noise sensitivity, it may adversely affect online operation and risk violating the linearity conditions required for accurate impedance measurement.

Recent studies have demonstrated the discrete-interval binary sequence (DIBS) as an effective alternative to PRBS for online battery impedance measurement [12], [13]. DIBS is a computer-optimized broadband binary signal that concentrates signal power at user-defined harmonic frequencies without increasing its time-domain amplitude. Compared to conventional PRBS, DIBS achieves significantly greater noise tolerance at selected frequencies while preserving the same low-amplitude profile. It retains all the advantages of PRBS, such as cost-effective implementation and fast measurement, while providing improved measurement quality in noisy environments.

The optimization procedure for synthesizing the DIBS can be summarized as follows [21]–[24].

- 1) *Specification*: Select the sequence length, bandwidth and the amplified frequencies inside the bandwidth.
- 2) *Initialization*: Start with a random binary sequence, obtain the phase angle in the frequency domain.
- 3) *Adjustment*: Form a new Fourier Transform sequence by using the phase angle and the user-defined spectral amplitude.
- 4) *Normalization*: Apply Inverse Fourier Transform to the newly formed sequence and collect only the signs of the time-domain sequence in order to form a new binary sequence, then apply Fourier Transform to convert the binary sequence back to the frequency domain.
- 5) *Iteration*: Repeat step 2 until the phase angle sequence remains unchanged.
- 6) *Result*: The last binary sequence obtained in the iterations becomes the optimal DIBS.

C. Battery health estimation

This work proposes a practical approach to battery SOH estimation using linear regression in combination with real-time battery impedance measurements. The ultimate goal is to develop a predictive model capable of estimating battery SOH based on measured impedance and known state parameters, as formulated in (1).

$$\hat{H} = f(Z, C, T) \quad (1)$$

In (1), f represents the SOH estimation function, \hat{H} denotes the estimation outcome, Z denotes the measured impedance spectra of the battery at a given condition, C denotes the battery SOC level and T denotes the battery temperature.

The construction of the estimation function f is guided by the following propositions. First, the growth of the SEI layer is correlated with an increase in the internal resistance of the battery cell across a continuous range of frequencies. Second, linear relationships between battery impedance and capacity loss are observed and remain consistent across cells with the same chemical composition. Third, each discrete frequency point in the impedance spectrum can be treated as an independent health indicator, each associated with its own linear model.

The proposed method consists of two stages: modeling stage and deployment stage. A linear regression analysis is applied in the modeling stage to select optimal battery indicators and build the prediction models while online impedance measurement is applied in the deployment stage to estimate the battery SOH using the built models. The DIBS is applied to all impedance measurements in both stages.

The modeling stage aims to produce a set of SOH estimation models and consists of the following steps.

- *Data collection*: An aging experiment is performed. Impedance and capacity performance test results are collected at each aging stage at various SOC and temperature conditions.
- *Data preprocessing*: Reference SOH values and the real part of the impedance spectra from each state condition are calculated from the performance test results, as shown in (2) and (3), respectively, where k denotes the k -th harmonic of the applied DIBS.

$$\text{SOH} = \frac{\text{Current capacity}}{\text{Rated capacity}} \times 100\% \quad (2)$$

$$R_k = \text{Re}\{Z_k\} \quad (3)$$

- *Model fitting*: Least-square fitting method is applied to obtain parameters for SOH prediction linear models based on impedance values, as shown in (4), where β_k and ϵ_k are the linear model parameters corresponding to the k -th harmonic of the applied DIBS.

$$\hat{Y}_k = \beta_k R_k + \epsilon_k \quad (4)$$

- *Model evaluation*: The coefficient of determination (R^2 index) is used to evaluate the fitting performance of the obtained linear models.
- *Model selection*: Select an optimal range of frequency in which the R^2 index shows consistently high value across cells. Collect the harmonic indexes of the DIBS harmonics inside the selected frequency range, denoted as K_{opt} . The parameters of the models associated with the selected optimal harmonics are stored in a lookup table.

In the deployment stage, the built models are applied to estimate the battery SOH in real time. The DIBS is used to perform online impedance measurements, which leverages all

the benefits of the signal such as fast measurement, noise-resistant and minimal disturbance to online battery operation. The estimation process consists of the following steps.

- *Measurement*: The battery impedance is measured online by applying the DIBS. Battery temperature and SOC are measured using onboard sensors or estimated by the battery management system.
- *Feature extraction*: Impedance real-part values at the optimal harmonic frequencies are extracted from the measurement.
- *SOH estimation*: Linear models corresponding to the measured battery SOC and temperature state condition are loaded and used along with the impedance measurement to estimate the battery SOH. The estimation outcomes from all the harmonics are combined by the use of averaging, as given in (5), to compute the final estimation result.

$$\hat{H} = \frac{1}{|K_{\text{opt}}|} \sum_{k \in K_{\text{opt}}} \hat{Y}_k \quad (5)$$

where \hat{Y}_k represents the estimation output at the k -th harmonic of the applied DIBS excitation.

IV. EXPERIMENTS

A. Experiment setup

An aging experiment was conducted on four commercial Li-ion battery cells (labeled C1, C2, C3, and C4) of the same manufactured model (INR21700-40T). The cathode material of the cells was nickel manganese cobalt dioxide (Li-NiMnCoO₂). The rated capacity of the cells was 4000 mAh. The experiment was accelerated by cycling the cells inside temperature-controlled chambers. Cells C3 and C4 were cycled at an elevated temperature of 35 °C, while cells C1 and C2 were cycled at 15 °C. The cycling followed a standard electric vehicle working cycle profile during the discharge phase and a constant-current constant-voltage (CC-CV) charging method during the charge phase (CC 2 A, CV 4.2 V). The experiment lasted for 400 cycles for cells C3 and C4, resulting in a 20% capacity loss by the end. Cells C1 and C2 were aged up to 200 cycles, reaching approximately 90% SOH at the conclusion of the experiment.

Reference performance tests were conducted for each cell at the beginning of the experiment and at every 200 cycles of accelerated aging. Cells C3 and C4 were additionally tested at cycle 100. The performance tests include charge capacity measurement and internal impedance measurement. Both capacity and impedance tests were conducted at various temperature set points: 15 °C, 25 °C and 35 °C. To ensure temperature stability, the cells were allowed to rest in the temperature-controlled climatic chamber for two hours before each test. In addition, at each test temperature, impedance measurements were conducted at various SOC conditions: 10%, 30%, 50%, 70% and 90%.

A measurement setup based on Fig. 2 was constructed to perform impedance measurements at all the test conditions.

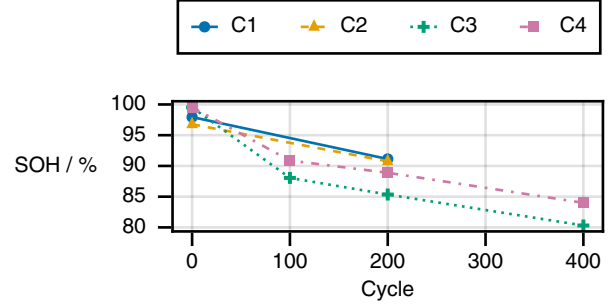


Fig. 3: Reference SOH of all cells during the aging experiment (capacity measured at 25 °C).

The DIBS was applied to measure the cell impedance within the frequency range 0.1 Hz to 2 kHz. The DIBS excitation amplitude was set to 250 mA and 35 harmonic frequencies were logarithmically selected inside the measurement band including the DIBS fundamental frequency. The DIBS was optimized in order to obtain accurate impedance measurements at the chosen frequencies.

B. Experimental results

Fig. 3 shows the progression of the SOH state parameter of all the cells during the cycling experiment. The reference SOH was calculated based on the capacity measurement at 25 °C, according to (2). As can be seen in Fig. 3, cycling the cells at an elevated temperature (45 °C for cells C3 and C4) results in a quicker loss of capacity, compared to the cycling at a lower temperature (15 °C for cells C1 and C2).

Fig. 4 presents the impedance measurements of cell C3 at different aging stages at 70% SOC and 25 °C temperature. As seen in the Nyquist plot, the effect of aging has resulted in the expansion of the semicircle arc most notably in the lower part of the frequency range (less than 100 Hz). It is useful to plot the real part of the impedance spectra at different cycling stages, as shown in Fig. 5. It can be seen that the lower part of the real-part impedance spectra (less than 10 Hz) shows more aggressive changes during the aging process.

C. Health estimation: least-square fitting

The obtained SOH and real-part impedance values were used to build SOH prediction models at various frequencies according to (4). A least-square method was applied to fit the impedance values to the SOH values for the training dataset consisting of cells C1, C3 and C4. Fig. 6 shows examples of the fitted linear models between the SOH and the real part of the cell impedance at various frequencies for cell C3 at 70% SOC and 25 °C temperature.

The coefficient of determination R^2 which describes the fidelity of a linear regression model on a dataset was used to evaluate the performance of the fitted linear regression models. Fig. 7 shows the R^2 index values at various frequencies of cells C3 and C4 validated against their own measurement data. The

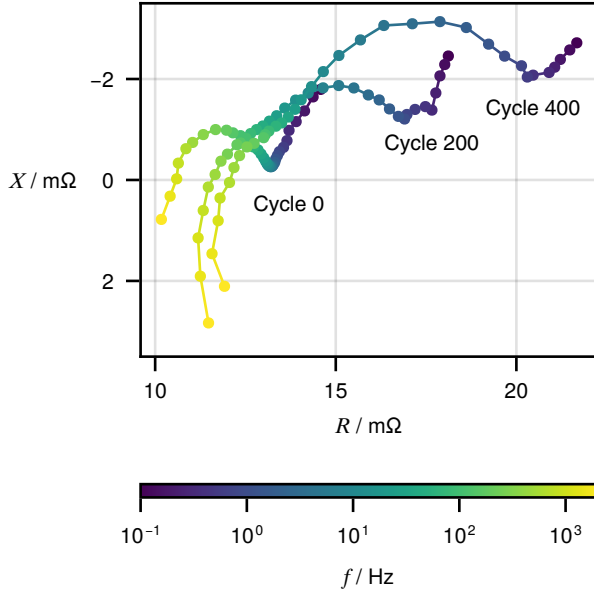


Fig. 4: Battery impedance spectra of cell C3 measured with the DIBS technique at various stages of cycling at 70% SOC and at room temperature 25 °C.

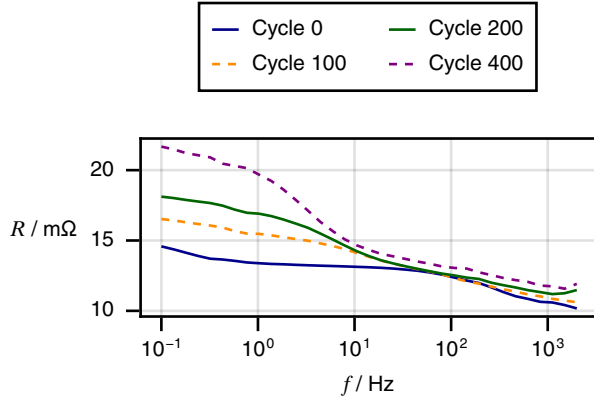


Fig. 5: Real part of the battery impedance spectra of cell C3 measured with the DIBS technique at various stages of cycling at 70% SOC and at room temperature 25 °C.

results show that the R^2 index is consistently high (above 0.8) for the frequencies less than 10 Hz, suggesting a strong predictive performance in this frequency range.

Based on the observations, a frequency range of 1 Hz to 5 Hz was selected as the optimal range for input feature extraction. The fitted linear models in such frequency range were extracted for each cell at 70% SOC and 25 °C. The model parameters from each cell are combined and averaged to produce a set of cell-averaged linear models parameters for each DIBS harmonic frequency in the frequency range 1 Hz

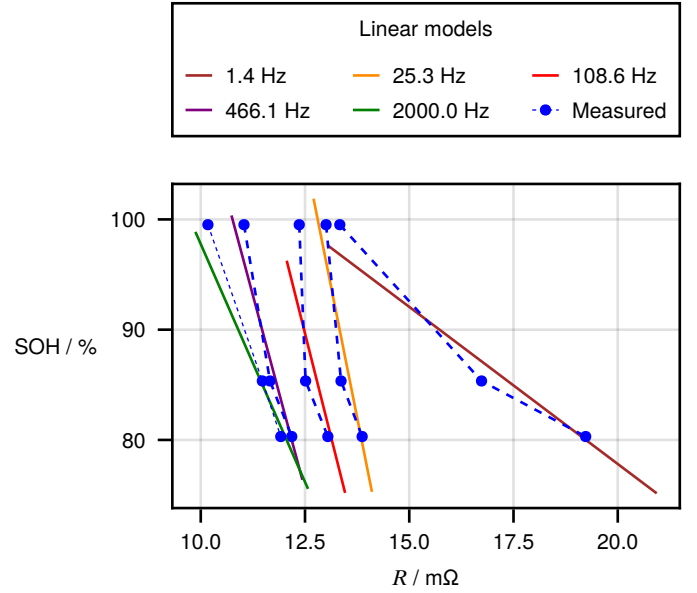


Fig. 6: Linear model fitting between the cell SOH and the real part of the measured impedance at various frequencies for cell C3 at 70% SOC and 25 °C temperature.

Frequency (Hz)	β	ϵ
1.03	-36.38	1.46
1.38	-37.86	1.48
1.84	-40.98	1.52
2.46	-45.07	1.57
3.3	-51.45	1.66
4.41	-60.82	1.78

TABLE I: Averaged SOH-prediction linear model parameters between 1 Hz and 5 Hz applicable for 70% SOC and 25 °C temperature conditions.

to 5 Hz. Table I shows the linear coefficients of the average models inside the optimal frequency range.

D. Estimation results at a single SOC and temperature

Cycle	SOH (%)	SOH estimation (%)	Absolute error (%)
0	96.78	96.91	0.13
200	90.75	90.6	0.15

TABLE II: SOH estimation results of cell C2 at a single SOC at 25 °C.

The effectiveness of the built models were tested against a test dataset consisting of cell C2. The obtained averaged linear models parameters were applied to estimate the SOH of the test cell (C2) at 70% SOC and 25 °C temperature. Table II shows the estimation values along with the absolute error deviation for cycle 0 and 200. The average absolute error of

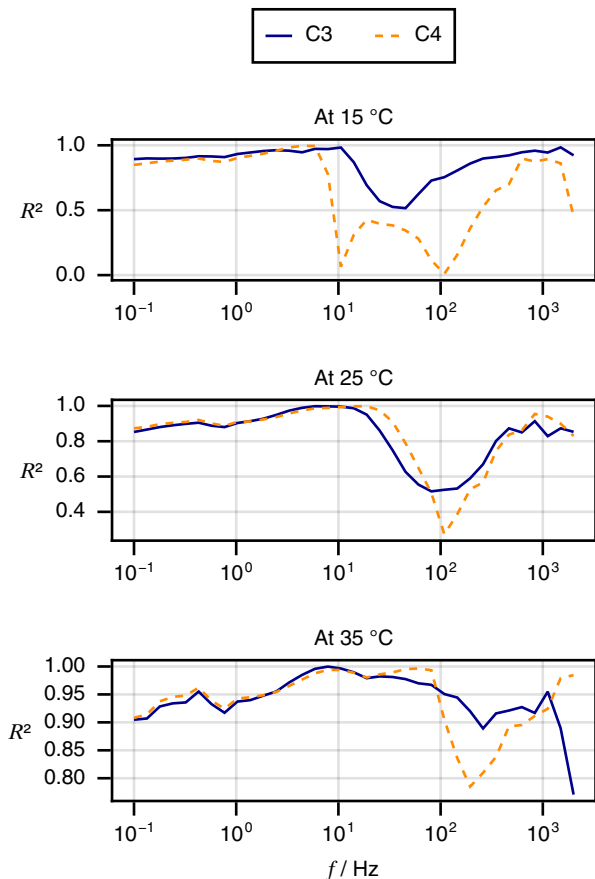


Fig. 7: R^2 index of SOH-impedance linear fitting for cells C3 (blue) and C4 (orange) from self validation at various temperatures.

the estimation was 0.14%. It is noted that by selecting 1 Hz as the lower end of the optimal frequency range, the measurement time of the applied DIBS in the deployment stage is reduced to only 3 seconds.

E. Estimation results at various SOC values and temperatures

Temperature	SOC				
	10%	30%	50%	70%	90%
15 °C	0.28	1.09	1.07	0.79	1.2
25 °C	0.74	0.43	0.21	0.14	0.77
35 °C	1.44	1.35	1.28	1.15	0.99

TABLE III: Absolute SOH estimation errors of cell C2 at multiple SOC and temperature conditions.

The optimal linear models parameters were applied to estimate the SOH of test cell C2 at various SOC values between 10% and 90% and various temperatures between 15 °C and 35 °C. Table III shows the deviation error values of the estimation at each temperature and SOC condition. The measured

SOH values at cycle 0 and 200 were used as reference values for error calculation. The prediction errors were averaged across the cycles for each SOC point and temperature value. Table III shows that the selected linear models are able to estimate battery SOH at various SOC values and temperatures with a high level of accuracy, although the estimation error slightly increases at both lowered temperature (15 °C) and elevated temperature (35 °C). An average estimation error of around 0.86% across all SOC and temperature conditions was obtained from the test results.

V. CONCLUSIONS

The battery SOH is a critical parameter which has a significant impact on safety and performance of Li-ion batteries. Studies have shown a strong relationship between the battery impedance and battery SOH. The recently proposed DIBS technique can be applied to quickly and accurately measure the battery impedance from which the SOH of a battery cell can be rapidly estimated online without relying on complex modeling techniques.

This paper has demonstrated the application of the battery impedance measured using the DIBS method in determining the SOH of a commercial Li-ion battery cell. Experimental measurements were carried out and analyzed to show the effectiveness of the method. An average SOH estimation error of 0.86% have been obtained by applying regression techniques to a wide temperature interval ranging from 15 °C to 35 °C. The estimation performance varies slightly depending on the cell temperature and SOC.

REFERENCES

- [1] G. Zubi et.al, "The lithium-ion battery: State of the art and future perspectives," *Renewable and Sustainable Energy Reviews*, vol. 89, pp. 292–308, 2018.
- [2] B. Gou, Y. Xu, and X. Feng, "An ensemble learning-based data-driven method for online state-of-health estimation of lithium-ion batteries," *IEEE Transactions on Transportation Electrification*, vol. 7, no. 2, pp. 422–436, 2020.
- [3] M. Bercibar, I. Gandiaga, I. Villarreal, N. Omar, J. Van Mierlo, and P. Van den Bossche, "Critical review of state of health estimation methods of li-ion batteries for real applications," *Renewable and Sustainable Energy Reviews*, vol. 56, pp. 572–587, 2016.
- [4] A. Basia, Z. Simeu-Abazi, E. Gascard, and P. Zwolinski, "Review on state of health estimation methodologies for lithium-ion batteries in the context of circular economy," *CIRP Journal of Manufacturing Science and Technology*, vol. 32, pp. 517–528, 2021.
- [5] S. B. Sarmah, P. Kalita, A. Garg, X.-d. Niu, X.-W. Zhang, X. Peng, and D. Bhattacharjee, "A review of state of health estimation of energy storage systems: Challenges and possible solutions for futuristic applications of li-ion battery packs in electric vehicles," *Journal of Electrochemical Energy Conversion and Storage*, vol. 16, no. 4, p. 040801, 2019.
- [6] M. C. et.al, "Use of impedance spectroscopy for the estimation of li-ion battery state of charge, state of health and internal temperature," *Journal of the Electrochemical Society*, vol. 168, no. 8, p. 080517, 2021.
- [7] C. Li, L. Yang, Q. Li, Q. Zhang, Z. Zhou, Y. Meng, X. Zhao, L. Wang, S. Zhang, Y. Li *et al.*, "Soh estimation method for lithium-ion batteries based on an improved equivalent circuit model via electrochemical impedance spectroscopy," *Journal of Energy Storage*, vol. 86, p. 111167, 2024.
- [8] M. Galeotti, L. Cinà, C. Giammanco, S. Cordiner, and A. Di Carlo, "Performance analysis and soh (state of health) evaluation of lithium polymer batteries through electrochemical impedance spectroscopy," *Energy*, vol. 89, pp. 678–686, 2015.

- [9] J. Sihvo, D.-I. Stroe, T. Messo, and T. Roinila, "Fast approach for battery impedance identification using pseudo-random sequence signals," *IEEE transactions on power electronics*, vol. 35, no. 3, pp. 2548–2557, 2019.
- [10] E. Locorotondo, S. Scavuzzo, L. Pugi, A. Ferraris, L. Berzi, A. Airale, M. Pierini, and M. Carello, "Electrochemical impedance spectroscopy of li-ion battery on-board the electric vehicles based on fast nonparametric identification method," in *Proc. IEEE International Conference on Environment and Electrical Engineering and IEEE Industrial and Commercial Power Systems Europe*, 2019, pp. 1–6.
- [11] A. Fairweather, M. Foster, and D. Stone, "Battery parameter identification with pseudo random binary sequence excitation (prbs)," *Journal of Power Sources*, vol. 196, no. 22, pp. 9398–9406, 2011.
- [12] M. Tran and T. Roinila, "Online impedance measurement of lithium-ion battery: Applying broadband injection with specified fourier amplitude spectrum," *IEEE Transactions on Industry Applications*, 2023.
- [13] A. Y. Kallel, A. Fischer, and O. Kanoun, "Discrete interval binary sequence for stable and stationary impedance spectroscopy of li-ion batteries," *IEEE Transactions on Instrumentation and Measurement*, 2023.
- [14] X. Wang, X. Wei, J. Zhu, H. Dai, Y. Zheng, X. Xu, and Q. Chen, "A review of modeling, acquisition, and application of lithium-ion battery impedance for onboard battery management," *eTransportation*, vol. 7, pp. 1–21, 2021.
- [15] A. Barré, B. Deguilhem, S. Grolleau, M. Gérard, F. Suard, and D. Riu, "A review on lithium-ion battery ageing mechanisms and estimations for automotive applications," *Journal of Power Sources*, vol. 241, pp. 680–689, 2013.
- [16] S. J. An, J. Li, D. Mohanty, C. Daniel, B. J. Polzin, J. R. Croy, S. E. Trask, and D. L. Wood, "Correlation of electrolyte volume and electrochemical performance in lithium-ion pouch cells with graphite anodes and nmc532 cathodes," *Journal of The Electrochemical Society*, vol. 164, no. 6, p. A1195, 2017.
- [17] S. J. An, J. Li, C. Daniel, H. M. Meyer III, S. E. Trask, B. J. Polzin, and D. L. Wood III, "Electrolyte volume effects on electrochemical performance and solid electrolyte interphase in si-graphite/nmc lithium-ion pouch cells," *ACS Applied Materials & Interfaces*, vol. 9, no. 22, pp. 18 799–18 808, 2017.
- [18] J. Wang, J. Purewal, P. Liu, J. Hicks-Garner, S. Soukazian, E. Sherman, A. Sorenson, L. Vu, H. Tataria, and M. W. Verbrugge, "Degradation of lithium ion batteries employing graphite negatives and nickel-cobalt-manganese oxide+ spinel manganese oxide positives: Part 1, aging mechanisms and life estimation," *Journal of Power Sources*, vol. 269, pp. 937–948, 2014.
- [19] M. Ecker, N. Nieto, S. Käbitz, J. Schmalstieg, H. Blanke, A. Warnecke, and D. U. Sauer, "Calendar and cycle life study of li (nmc) o2-based 18650 lithium-ion batteries," *Journal of Power Sources*, vol. 248, pp. 839–851, 2014.
- [20] D. D. Macdonald, "Reflections on the history of electrochemical impedance spectroscopy," *Electrochimica Acta*, vol. 51, no. 8-9, pp. 1376–1388, 2006.
- [21] A. V. D. BOS and R. Krol, "Synthesis of discrete-interval binary signals with specified fourier amplitude spectra," *International Journal of Control*, vol. 30, no. 5, pp. 871–884, 1979.
- [22] M. Buckner and T. Kerlin, "Optimum binary signals for reactor frequency response measurements," *Nuclear Science and Engineering*, vol. 49, no. 3, pp. 255–262, 1972.
- [23] K.-D. Paehlike and H. Rake, "Binary multifrequency signals - synthesis and application," *IFAC Proceedings Volumes*, vol. 12, no. 8, pp. 589–596, 1979.
- [24] S. L. Harris and D. A. Mellichamp, "On-line identification of process dynamics: use of multifrequency binary sequences," *Industrial & Engineering Chemistry Process Design and Development*, vol. 19, no. 1, pp. 166–174, 1980.